Dynamical Decomposition of Low-Frequency Tendencies

MING CAI

Cooperative Institute for Climate Studies, Department of Meteorology, University of Maryland, College Park, Maryland

HUUG M. VAN DEN DOOL

Climate Analysis Center, National Meteorological Center, Washington, D.C.

(Manuscript received 16 August 1993, in final form 10 December 1993)

ABSTRACT

A nearly complete vorticity equation is used to diagnose the tendency components of the low-frequency variations of the 500-mb streamfunction induced by various internal linear–nonlinear interaction processes. With the aid of a special composite technique ("phase-shifting" method) that effectively records the observations in a coordinate system moving with an identifiable low-frequency pattern, the authors are able to separate the internal interactions that primarily act to make low-frequency waves propagate from those that are mostly responsible for development/maintenance/decay ("maintenance" for brevity) of low-frequency transients. It is found that the low-frequency transients are maintained primarily by two nonlinear interaction processes: one is the vorticity flux of high-frequency eddies and the other is the interaction of low-frequency transients and stationary waves. It is also found that an individual propagation tendency component may be much larger than a maintenance tendency component. In particular, the beta effect and the advection of the low-frequency vorticity by the zonally averaged climatological wind are the dominant terms among the propagation tendency components. But there is a great deal of cancellation among the propagation tendency components. As a result, the net magnitude of the tendency components describing propagation is only slightly larger than those relating to maintenance of low-frequency waves. From a forecast point of view, both propagation and forcing terms are equally important if an accurate forecast beyond a few days is required.

1. Introduction

The central problem in numerical extended-range weather prediction is to account for the atmospheric low-frequency variability with periods beyond the cyclone time scale. Both for diagnostics and prediction studies, one of the important aspects of low-frequency variability is the tendency field of low-frequency transients. Because the time scale of low-frequency transients is usually defined in a geographically fixed coordinate system, the tendency field would naturally consist of two parts: (i) development/maintenance/decay (change in amplitude, or briefly, "maintenance") and (ii) propagation (change in the position of ridges or troughs). Documentation of the tendency field of low-frequency variation in terms of maintenance versus propagation would help us to determine what makes low-frequency waves be low frequency: that is, are they (i) slowly amplifying/decaying stationary oscillators and/or (ii) slowly traveling mobile waves?

The issue of the tendency of low-frequency variations has been addressed most often in terms of only one single tendency component, namely, the tendency (or barotropic feedback) induced by the vorticity flux of the high-frequency eddies. It has become customary to study interaction of low-frequency variability and high-frequency eddies by examining the spatial relation between low-frequency flow and the feedback of high-frequency eddies (Green 1977; van den Dool 1982; Shutts 1983; Hoskins et al. 1983; Holopainen and Fortelius 1987; Metz 1987, 1990, 1991; Lau 1988; Cai and van den Dool 1991, 1992; Lau and Nath 1991). We should point out here that the resemblance between low-frequency flow and the barotropic feedback does not, in itself, mean that low-frequency flow is the response to the tendency induced by vorticity flux of high-frequency eddies. The total tendency in low-frequency waves is determined by the sum of many terms, and the so-called feedback of high-frequency eddies is only one of them, as shown in the equation below, a symbolic equation for the tendency of the low-frequency component of an atmospheric variable (say, 500-mb streamfunction ψ),

$$\frac{\partial \psi^L}{\partial t} = \chi_{hf} + \chi_1 + \cdots + \chi_n + \text{others}. \quad (1)$$

In (1), χ_{hf} denotes the feedback of high-frequency eddies; χ_j stands for the tendency component induced by

Corresponding author address: Dr. Ming Cai, CICS, Department of Meteorology, University of Maryland, College Park, MD 20742.

other internal interaction terms; and "others" stands for the tendency component induced by yet other mechanisms, such as the external forcings and dissipation. Using (1) alone as guidance, one would expect the tendency due to high-frequency eddies (χ_{hf}) to resemble the observed tendency in low-frequency flow ($\partial\psi^L/\partial t$) rather than the low-frequency anomaly itself (ψ^L), as found in the references given earlier. This argument was also pointed out by Higgins and Schubert (1993). It is precisely here where the "maintenance" versus propagation question has to be asked. The internal interaction terms in (1) include (i) the linear interaction between the time mean flow and low-frequency waves, (ii) nonlinear interactions among low-frequency waves as well as between low- and high-frequency transients, and (iii) the interaction among high-frequency eddies (i.e., the feedback of high-frequency eddies). The feedback of high-frequency transients (χ_{hf}) is actually one of the smallest terms among those internal interaction terms, as we shall show later in this paper. It remains therefore to be clarified why a single term (the feedback of high-frequency eddies) alone could be of so much importance for the atmospheric low-frequency variability, and why its spatial patterns resemble low-frequency anomalies (ψ^L).

Cai and Van den Dool (1991, 1992; hereafter referred to as CD1 and CD2, respectively) used a so-called phase-shifting method to identify the spatially coherent relation between low-frequency waves and the low-frequency component of the tendency induced by high-frequency eddies. Here we want to extend our previous diagnostic analysis by examining all tendency terms derived from the vorticity equation for low-frequency flow. Our general goal is to determine the relation between the observed tendency of low-frequency flow (which consists of both propagation and maintenance components) and the tendency components induced by each of the individual interaction terms in the vorticity equation. We are particularly interested in whether the internal interaction terms are related more to the observed tendency ($\partial\psi^L/\partial t$) or to the observed low-frequency waves (ψ^L) themselves. Obviously, internal processes that primarily account for propagation of low-frequency waves would play little role in terms of providing energy to low-frequency waves (which is not to say that they are unimportant for forecasting). However, those processes that contribute little to the observed tendency but have good spatial correlation with low-frequency waves themselves may act to "maintain"/"damp" low-frequency waves by providing/drawing energy to/from them because the energy generation term is proportional to $\psi^L\chi_j$ instead of $(\partial\psi^L/\partial t)\chi_j$, where χ_j is the tendency component evaluated from a term on the right-hand side of the vorticity equation. The key appears to be the distinction between time tendencies due to propagation on the one hand and amplitude growth or decay on the other. By doing so, we are able to tell which processes primarily cause low-frequency waves to move and which are primarily responsible for maintaining low-frequency waves. The phase-shifted coordinate discussed in CD1 and CD2 is naturally suitable for distinguishing propagation versus maintenance.

Using a linear version of the NCAR GCM model (CCM), Branstator (1992) has investigated the atmospheric responses to the tendency components induced by various mechanisms. He attempts to relate these linear steady solutions to the prominent low-frequency (EOF) patterns found in a 6000-day perpetual January integration with the full CCM. Because of the nature of the steady solution as well as the EOF analysis that can only describe the "stationary oscillatory" low-frequency patterns, the propagation part of low-frequency variability was essentially left untouched or "aliased" into geographically fixed patterns. In the present study, we use the phase-shifting method to examine the relation between low-frequency waves, their observed tendency, and the tendency components induced by all internal interaction terms identified in the framework of a nearly complete vorticity equation (see section 3 for details). As will be shown in this paper, the phase-shifting method is capable of identifying both the terms that act to maintain low-frequency waves (e.g., the positive feedback of high-frequency eddies as found in CD1) and the terms that are responsible for the propagation of low-frequency waves.

We begin our presentation with a brief description of the data used in this study. Section 3 defines the tendency terms derived from the vorticity equation for low-frequency flow. Section 4 contains the standard deviations of these tendency components and the temporal correlation maps between the observed tendency and the sum of the calculated tendency components. These simple statistics would give the readers an idea of the amplitude of an individual tendency component and its relative importance in giving rise to the observed (total) tendency. Section 5 presents the mean tendency fields calculated from four coordinate frames that move around with low-frequency waves with wavenumbers 1–4. The maps presented in this section address the issue of propagation versus maintenance of low-frequency waves and the roles of an individual dynamical process in changing the atmospheric low-frequency waves. Conclusions of our findings are given in section 6.

2. Data

The data used in this study are wintertime Northern Hemisphere twice daily 500-mb wind derived from European Centre for Medium-Range Weather Forecasts (ECMWF) analysis, available in the data archives of the National Center for Atmospheric Research. Six winter seasons from 1985/86 to 1990/91 are considered. Each winter season is taken to be a 150-day period and starts 15 October of the first year. The data

are stored on a 2.5° × 2.5° latitude–longitude grid covering the area from the equator to the North Pole.

A simple temporal harmonic technique is used to separate the low-frequency fluctuations from the high-frequency eddies. Specifically, the data at each grid point in each winter season are temporally decomposed in the frequency domain ω_n, where $\omega_n = 2\pi n/150$ day^{-1}, $n = 1, 2, \cdots, 150$. The low-frequency and high-frequency components of a variable "w" are then obtained as

$$w^{\mathrm{L}}(\lambda, \phi, t) = \sum_{n=1}^{22} [A_n(\lambda, \phi)\cos(\omega_n t) + B_n(\lambda, \phi)\sin(\omega_n t)],$$

$$w^{\mathrm{H}}(\lambda, \phi, t) = \sum_{n=23}^{150} [A_n(\lambda, \phi)\cos(\omega_n t) + B_n(\lambda, \phi)\sin(\omega_n t)], \quad (2)$$

where λ is longitude, ϕ is latitude, and t is time; A_n and B_n are the Fourier coefficients of the time series of the variable w at a grid point (λ, ϕ) in a given winter season. Therefore, the time series w^{L} at each grid consists of the fluctuations with periods between a week and a season, while w^{H} consists of the fluctuations with periods less than a week. The time mean $\bar{w}(\lambda, \phi)$ of the six winter seasons is determined as the average of the zero-frequency components of the six winters. One might argue that Eq. (2) is not a perfect filter since the time series of the atmospheric motion is by no means periodic. A filtering technique such as employed by Blackmon (1976) has better characteristics in this regard. In addition, our (or any other) definition of high- and low-frequency fluctuations is somewhat arbitrary. However, with broadband resolution sought, a spectral technique should be adequate to distinguish the fluctuations in high and low frequencies. As shown in CD1 and CD2, the variance maps of the transients obtained with our spectral technique have the same characteristics as those of other studies in spite of differences in the filtering technique and the precise definitions of the high- and low-frequency fluctuations.

3. Tendency equation

The derivation of the tendency equation for low-frequency flow starts with the conventional vorticity equation of the free atmosphere neglecting only the vertical advection and the twisting terms,

$$\frac{\partial \zeta}{\partial t} + \mathbf{v}\cdot\nabla(f + \zeta) + (f + \zeta)\nabla\cdot\mathbf{v} = 0, \quad (3)$$

where ζ is vorticity, t is time, $\mathbf{v}$ is wind (including the divergent component), and $f = 2\Omega\sin\varphi$ is the Coriolis parameter. We then decompose all quantities in Eq. (3) into time-mean, low-frequency, and high-frequency components according to (2) and derive the vorticity equation for the low-frequency flow as

$$\begin{aligned}\frac{\partial \zeta^{\mathrm{L}}}{\partial t} = &-\bar{\mathbf{V}}_r\cdot\nabla\zeta^{\mathrm{L}} - \mathbf{v}_r^{\mathrm{L}}\cdot\nabla\bar{\zeta} \\ &- \{\mathbf{v}_r^{\mathrm{L}}\cdot\nabla\zeta^{\mathrm{L}}\}^{\mathrm{L}} - \{\mathbf{v}_r^{\mathrm{H}}\cdot\nabla\zeta^{\mathrm{H}}\}^{\mathrm{L}} \\ &- \{\mathbf{v}_r^{\mathrm{L}}\cdot\nabla\zeta^{\mathrm{H}} + \mathbf{v}_r^{\mathrm{H}}\cdot\nabla\zeta^{\mathrm{L}}\}^{\mathrm{L}} - v_r^{\mathrm{L}}\frac{df}{ad\varphi} \\ &- f\nabla\cdot\mathbf{v}_d^{\mathrm{L}} - \left\{\nabla\cdot(\mathbf{v}_d\zeta) + v_d\frac{df}{ad\varphi}\right\}^{\mathrm{L}}, \quad (4)\end{aligned}$$

where the superscripts "L" and "H" refer to low- and high-pass filtering operators defined in (2), respectively, and the overbar means a six-winter mean. Here $\mathbf{v}_r$ and $\mathbf{v}_d$ are the rotational and divergent components of the wind, respectively. The variables in the last term on the right-hand side of (4) have not been subjected to the timescale decomposition. Applying a reverse Laplace operator on both sides of Eq. (4) yields the tendency equation for the low-frequency component of the streamfunction:

$$\chi_0 = \frac{\partial \psi^{\mathrm{L}}}{\partial t} = \chi_1 + \chi_2 + \chi_3 + \chi_4 + \chi_5 + \chi_6 + \chi_7 + \chi_8 + R, \quad (5)$$

where

$$\begin{aligned}\psi^{\mathrm{L}} &= \nabla^{-2}\zeta^{\mathrm{L}}, \\ \chi_1 &= \nabla^{-2}\{-[\bar{\mathbf{V}}_r]\cdot\nabla\zeta^{\mathrm{L}} - \mathbf{v}_r^{\mathrm{L}}\cdot\nabla[\bar{\zeta}]\}, \\ \chi_2 &= \nabla^{-2}\{-\bar{\mathbf{V}}_r^{*}\cdot\nabla\zeta^{\mathrm{L}} - \mathbf{v}_r^{\mathrm{L}}\cdot\nabla\bar{\zeta}^{*}\}, \\ \chi_3 &= \nabla^{-2}\{-\mathbf{v}_r^{\mathrm{L}}\cdot\nabla\zeta^{\mathrm{L}}\}^{\mathrm{L}}, \\ \chi_4 &= \nabla^{-2}\{-\mathbf{v}_r^{\mathrm{H}}\cdot\nabla\zeta^{\mathrm{H}}\}^{\mathrm{L}}, \\ \chi_5 &= \nabla^{-2}\{-\mathbf{v}_r^{\mathrm{L}}\cdot\nabla\zeta^{\mathrm{H}} - \mathbf{v}_r^{\mathrm{H}}\cdot\nabla\zeta^{\mathrm{L}}\}^{\mathrm{L}} \\ \chi_6 &= \nabla^{-2}\left\{-v_r^{\mathrm{L}}\frac{df}{ad\varphi}\right\}, \\ \chi_7 &= \nabla^{-2}\{-f\nabla\cdot\mathbf{v}_d^{\mathrm{L}}\}, \\ \chi_8 &= \nabla^{-2}\left\{-\nabla\cdot(\mathbf{v}_d\zeta) - v_d\frac{df}{ad\varphi}\right\}^{\mathrm{L}}. \quad (6)\end{aligned}$$

Term R represents the tendency of the rotational flow induced by other processes such as dissipation, external forcing, and the two neglected terms (i.e., vertical advection and twisting terms). Since we will evaluate R as a residue to balance Eq. (5), R also contains the accumulated errors associated with time–space truncation and analysis errors in the input fields. The bracket in the expression for χ_1 means a zonal averaging operator, and the asterisk in the expression for χ_2 means the zonal departure (or wavy) part of the

flow. The interpretation for terms on the rhs of (5) is straightforward. Here χ_1 is the tendency induced by the interaction between the low-frequency transients and the zonally symmetric component of the time mean flow, while χ_2 is the tendency due to the interaction of the low-frequency transients and the stationary waves; χ_3 and χ_4 are the tendencies resulting from the self-interaction among the low-frequency transients and among the high-frequency eddies, respectively; χ_5 is generated through the interaction between low- and high-frequency eddies; χ_6 essentially is a beta term and χ_7 is the tendency of the rotational flow induced by the stretching/converging effect of the irrotational flow; and χ_8 represents the ageostrophic effects of the motion.

There is some arbitrariness in our tendency decomposition, which comes fully or partly from one of three factors: (i) the definition for low- and high-frequency transients, (ii) separation of rotational wind from irrotational wind, and (iii) dividing the climatological circulation into zonally symmetric and asymmetric parts. As in all studies on low-frequency variability, there always exists arbitrariness in separating low-frequency transients from high-frequency transients because the temporal spectrum of atmospheric motion is continuous. In the papers of Blackmon, Wallace, and Lau (e.g., Blackmon 1976; Blackmon et al. 1977; Lau 1978; Wallace and Blackmon 1983), it has been well established that the atmospheric low-pass transients exhibit distinct spatial structure from that associated with the high-frequency eddies. The works of Hoskins et al. (1983) and Lau and Holopainen (1984) further set up a dynamical basis for the separation of low-frequency transients from high-frequency transients by showing the distinct relations with the climatological flow of the atmospheric transients with the two broad timescales. Most important, these distinct features are not very sensitive to a particular choice of criterion used in defining low- and high-frequency fluctuations. Hence, we tend to believe that the impact of our definition for low- and high-frequency fluctuations would be minimal in our tendency calculation. The decomposition of the total wind into rotational and divergent winds is done for somewhat historic reasons, as it allows us to interpret our results in the framework of quasigeostrophic theory (note that the first six tendency terms correspond to the barotropic vorticity equation, and these six terms together with χ_7 yield the potential vorticity equation of a shallow-water system). In light of the results of Simmons et al. (1983), further separating the time mean flow into the zonally symmetric and wavy parts would enable us to examine the role of the presence of the zonal asymmetry in the climatological mean flow in generating low-frequency variability.

All $\chi_j, j = 1$ to 8, can be readily calculated from the wind data. We evaluate χ_0, the observed tendency of the rotational flow, according to

$$\chi_0 = \frac{\partial \psi^L}{\partial t} = \frac{\psi^L(t + \Delta t) - \psi^L(t - \Delta t)}{2\Delta t}, \qquad \Delta t = 1/2 \text{ day} \quad (7)$$

except for the first time and the last time of each winter at which a forward or a backward finite-difference scheme is used instead. The one-day time step in evaluating χ_0 is quite consistent with the definition of the time scale of low-frequency transients (a week to a season). To put χ_0 on an equal footing with the individual tendency components χ_j's, we have divided χ_0 defined in (7) by a factor of 86 400 so that all of the tendency terms have a unit of meters squared per square second.

4. Statistics of the tendencies

This section reports some statistics of the terms in the tendency equation (5). Because the time mean of each χ_j is zero, the magnitude of a tendency term can be characterized by its standard deviation in time. The spatial patterns of the standard deviation of each of the tendency terms in Eq. (5) are somewhat like the familiar standard deviation map of low-frequency variability, exhibiting local maxima over the central regions of the North Pacific and North Atlantic Oceans, respectively (not shown here). To give the readers an idea about magnitude of each of the tendency terms, we list in Table 1 the hemispheric mean value of the standard deviation of the tendency terms. It is rather significant that except for the terms χ_4 and χ_5, all terms on the rhs of Eq. (5) have a comparable amplitude with the observed tendency (χ_0) itself, indicating that there must be a great deal of cancellation among the various tendency components. The three leading terms in the tendency equation are χ_6, χ_7, and χ_1, each of which is about twice as large as the observed tendency. One of the main points in this paper is that the term χ_4, which was often the only term that has been examined extensively by many investigators including ourselves, is actually the smallest term in the tendency equation. And yet, we will show in the next section that this term is one of the two terms that reinforce the low-frequency waves. It is of interest to point out that the standard

TABLE 1. Hemispheric mean values of the standard deviation of the tendency terms in Eq. (5) (in units of $m^2 s^{-2}$).

Term	Standard deviation	Term	Standard deviation
χ_0	30.39	χ_1	60.39
χ_2	29.93	χ_3	28.81
χ_4	11.74	χ_5	11.92
χ_6	73.48	χ_7	65.96
χ_8	40.22	R	40.89
$\sum_{j=1}^{8} \chi_j$	48.87		

deviations of both $\Sigma_{j=1}^{8} \chi_j$ and the residual term R are greater than that of the observed total tendency. This could be explained partly from the facts that χ_0 is a 24-h tendency (but normalized by 86 400 sec), whereas χ_j (j = 1 to 8) are instantaneous tendency components and that without the dissipation and external forcing terms, Eq. (5) by no means is a complete equation for the tendency of low-frequency transients. Nevertheless, we can conclude that if an accurate forecast of χ_0 is required (say error $\leq$10% of 30.39), no terms in (5) can be neglected.

Plotted in panel (a) of Fig. 1 is the temporal correlation map between the observed tendency χ_0 and the sum of the calculated tendencies χ_j, where j runs from 1 through 8. It is seen that the correlation is smaller than 0.8 everywhere but exceeds 0.6 in a middle-latitude band except for a region over the Eurasian continent where the correlation drops below 0.4. Again, the "nonperfect" (i.e., less than 100%) correlation is due partly to the fact that χ_0 is a 24-h tendency, whereas χ_j (j = 1 to 8) is an instantaneous tendency component. Of course, the processes not retained in the vorticity equation (3), such as indirect effects of the lower boundary forcings and dissipation, contribute partly to the "nonperfect" correlation as well. Also errors in the data used to calculate χ_j, j = 1 to 8, may be nonnegligible. Nevertheless, Fig. 1a shows how hard it is to forecast low-frequency tendencies accurately. Panel (b) of Fig. 1 is the temporal correlation between χ_0 and the sum of all the calculated tendencies except the terms χ_4 and χ_5 that involves the high-frequency transients. It is easily seen that there is a great similarity between the two maps, but the correlation shown in panel (b) is systematically smaller than the one shown in panel (a). This leads to the conclusion that although they are small, a sufficiently accurate evaluation of χ_4 and χ_5 would contribute significantly to the accuracy of forecasting χ_0.

5. Mean tendency fields of low-frequency waves

Cai and Van den Dool have used a phase-shifting method to identify the time mean maps of low-frequency waves and the tendency induced by high-frequency eddies (i.e., χ_4 in this paper). The phase-shifting method is a special composite analysis that follows an individual low-frequency wave of a reference field (say ψ^L) at a reference latitude (ϕ_0) in a frame moving with a speed equal to the instantaneous phase speed of that low-frequency wave. In such a moving frame, the traveling wave that we follow becomes stationary and the other (stationary and traveling) waves are nonstationary. As a result, only the wave that we follow will show up on the time-mean map of the reference field calculated in the moving frame. Moreover, we could deduce all kinds of statistics (just like we do in the geographically fixed coordinate) in the moving frame and examine the relation between the mean map of the reference field and the various statistics of other fields, such as the variability of high-frequency eddies (traveling storm tracks) and the feedback of high-frequency eddies in the same moving frame as we did in CD1. In

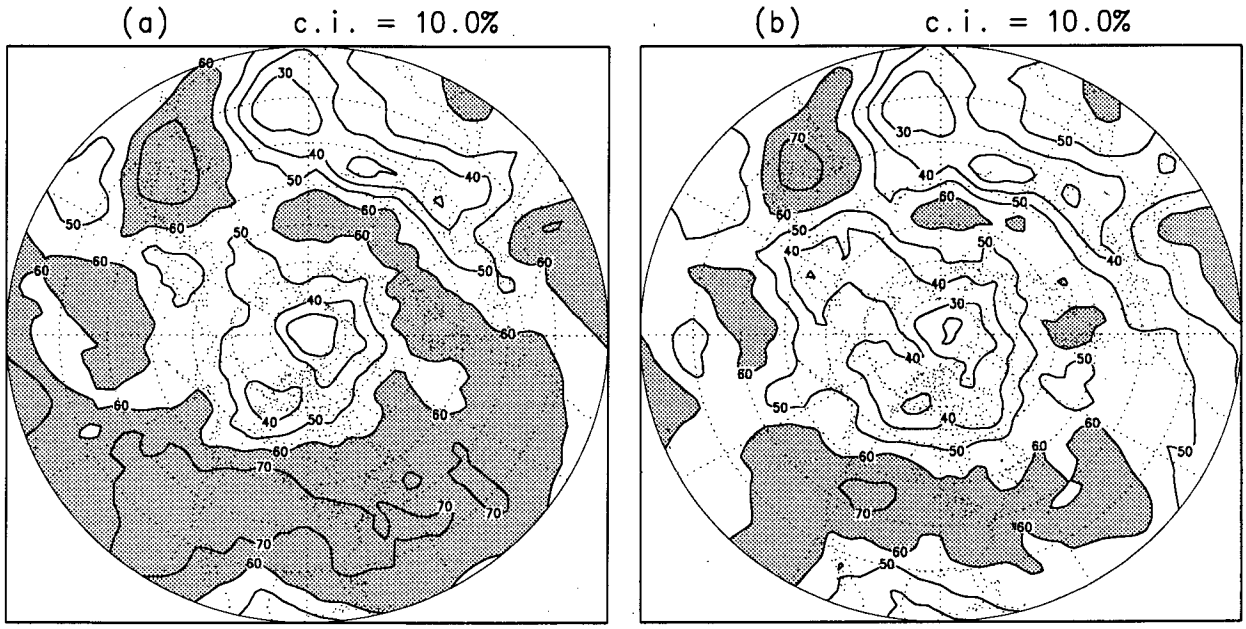

FIG. 1. Temporal correlation maps (a) between the observed tendency and the sum of the calculated tendency components and (b) between the observed tendency and the sum of the calculated tendency components excluding the components that involve high-frequency transients. The area with correlation larger than 60% has been shaded.

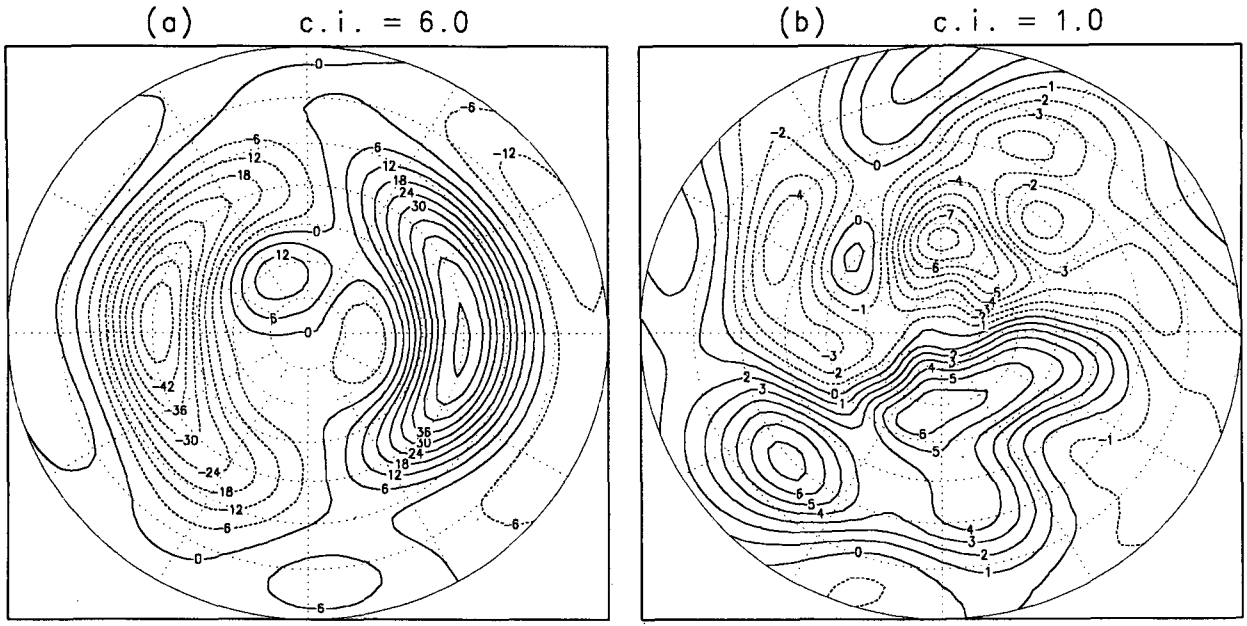

FIG. 2. Time-mean maps calculated in the moving frame $m = 1$: (a) the low-frequency streamfunction and (b) the observed tendency of the low-frequency streamfunction. The unit for (a) is 10^5 m^2 s^{-1} and for (b) m^2 s^{-2}.

this section, we present the ensemble mean maps of all tendency terms calculated in a frame that moves with an individual low-frequency wave. The objective is to examine the spatially coherent relation between the low-frequency waves and their observed tendencies and between the low-frequency waves and an individual tendency component calculated in the framework of vorticity dynamics. It should be pointed out here that unlike the works presented in CD1 and CD2, removing the stationary component from the data by using the phase-shifting method is no longer an issue in this study since all tendency terms defined in (6) and (7) have

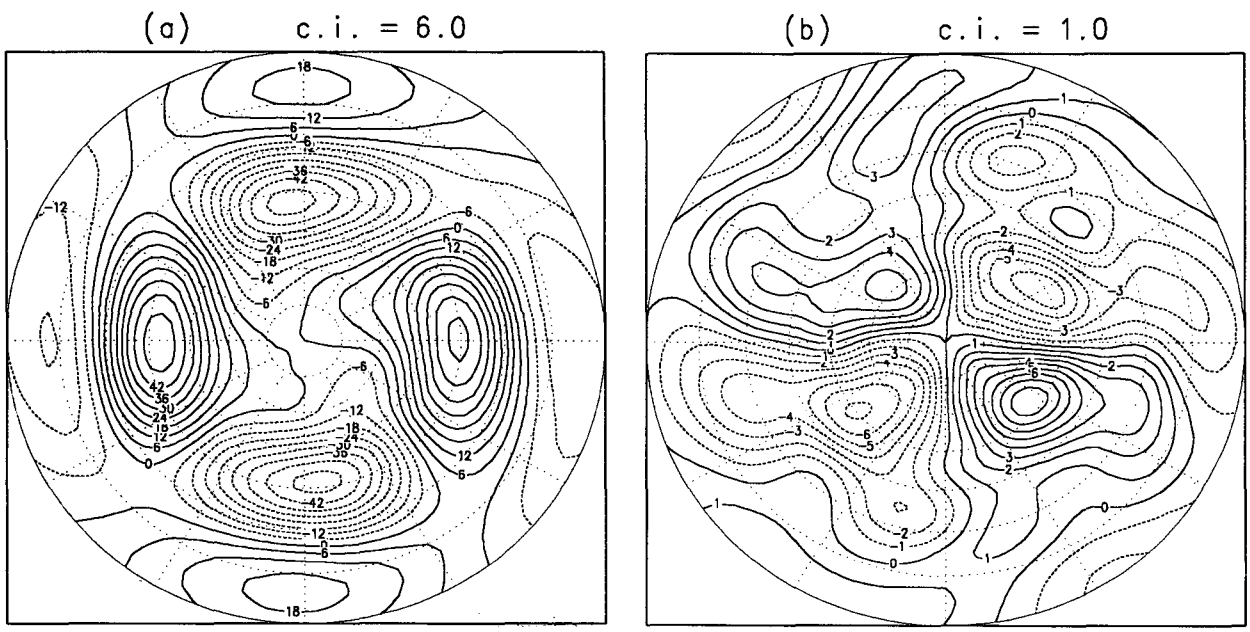

FIG. 3. As in Fig. 2 except for the moving frame $m = 2$.

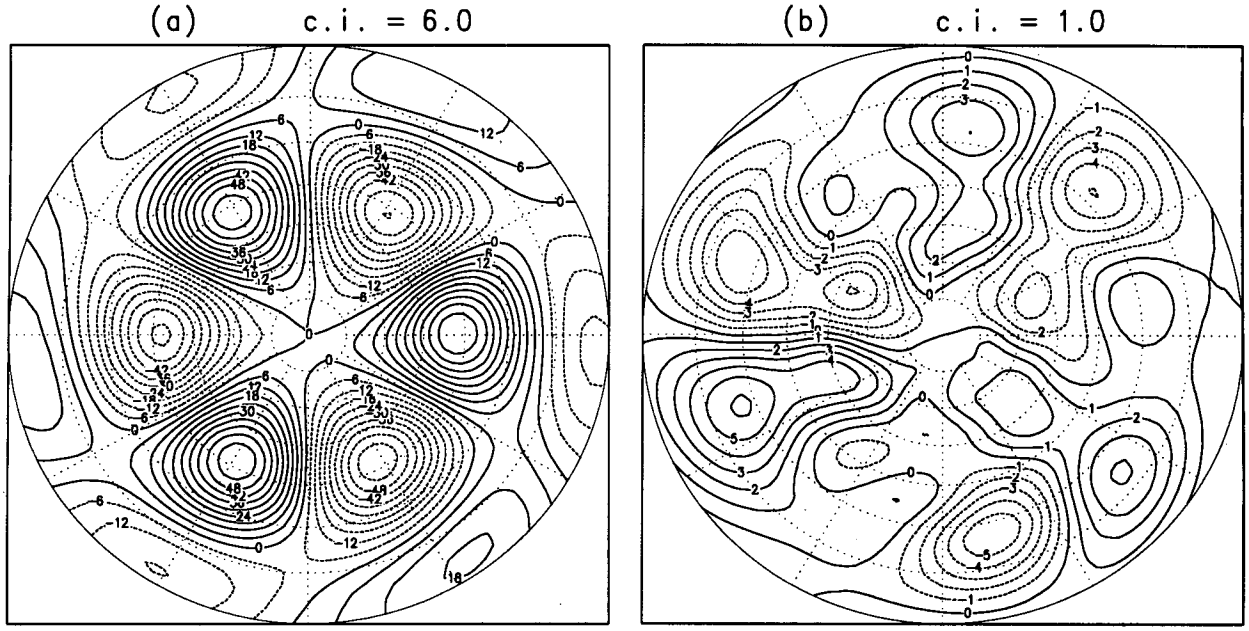

FIG. 4. As in Fig. 2 except for the moving frame $m = 3$.

zero mean (i.e., no stationary component). The use of the phase-shifting method enables us to determine the spatial relation between low-frequency waves and their associated tendencies.

As in our previous two papers, we have chosen the ridges of low-frequency waves $m = 1$, 2, 3, and 4 of the 500-mb streamfunction at 50°N as the targets to be followed in constructing the moving frames. Shown in Figs. 2–5 are the time mean maps of the low-frequency component of the streamfunction [panel (a)] and the observed tendency χ_0 [panel (b)] calculated in each of the moving frames $m = 1$, 2, 3, and 4. Since the ab-

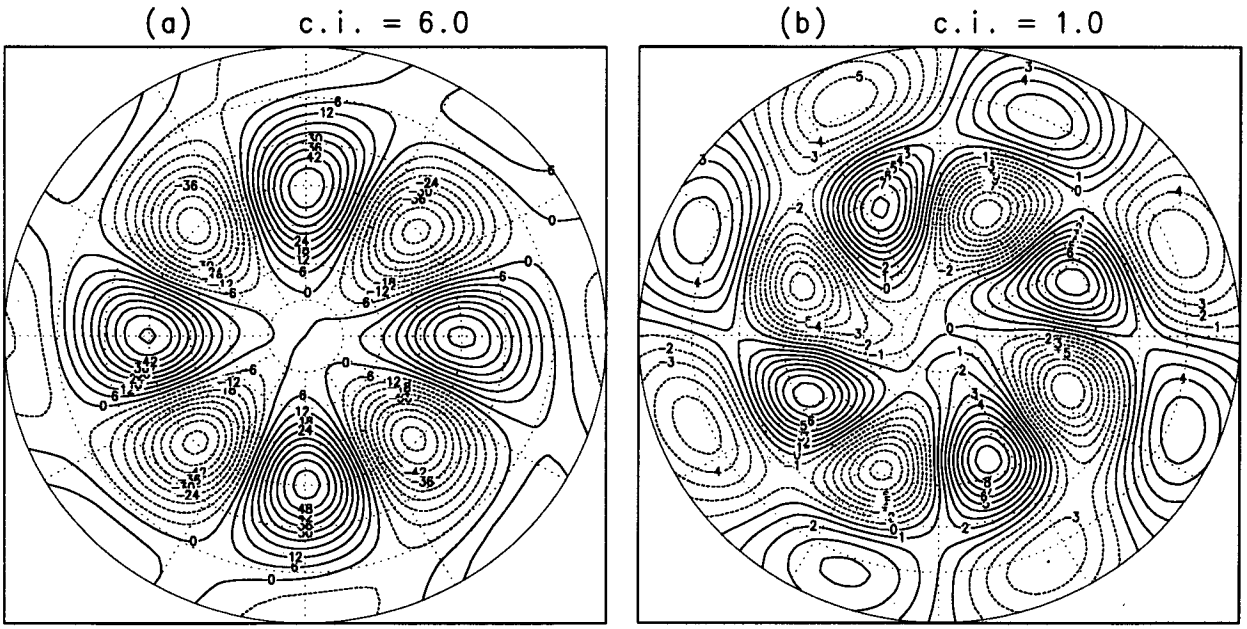

FIG. 5. As in Fig. 2 except for the moving frame $m = 4$.

solute geographic longitude of the troughs (or ridges) of a field are meaningless in a moving frame, we have removed the continent outline from the maps. The time mean maps of low-frequency waves ψ^L [panel (a) of Figs. 2–5] are supposed to be "identical" to the maps shown in panel (a) of Figs. 5–8 in CD1 except that here we used the streamfunction derived from six-winter ECMWF wind data instead of ten-winter NMC geopotential height. The maps shown in panel (a) of these four figures are used as a reference for examining the relation between low-frequency flow and its tendency χ_0. According to CD1, the time mean map of low-frequency waves obtained in a moving frame $m = m_0$ can be regarded as a proxy to the time mean structure of the traveling low-frequency wave with wavenumber $m = m_0$. It follows that we may then interpret the time mean tendency map calculated in the same moving frame as the time mean tendency associated with that particular low-frequency wave m_0.

Let us begin our discussion with the time mean maps obtained in the moving frame $m = 1$ (Fig. 2). It is seen that the pattern shown in the tendency map [panel (b)] is nearly orthogonal to the patterns of the low-frequency waves themselves [panel (a)]. This implies that the observed tendency associated with the low-frequency wave $m = 1$ in the mean primarily acts to move the low-frequency wave around. By comparing trough (or ridge) positions of these two maps, we can conclude that the low-frequency wave $m = 1$ would move westward in time. Another salient feature is that whereas the dominant wave in Fig. 2b is wavenumber one, other wave components also appear to be nontrivial. The appearance of other wave components in the mean tendency map is an empirical evidence of nonlinear interactions. Applying the time tendency in Fig. 2b, the nearly pure wavenumber one shown in Fig. 2a would transform over a short period (several days) to a configuration where $m = 1$ would become less dominant and other waves would emerge.

Examining the mean maps calculated in the moving frames $m = 2$, 3, and 4 (Figs. 3–5) also reveals the near-orthogonality between the low-frequency waves and their associated tendency fields. The low-frequency waves $m = 2$ and 3 shown in panel (a) of Figs. 3 and 4 would move toward the west since the ridges (or troughs) on the tendency maps [panel (b)] are about a quarter-wavelength west of the ridges (or troughs) of the corresponding low-frequency waves. In contrast, the low-frequency wave $m = 4$ shown in Fig. 5a tends to move east since the ridges (or troughs) of the tendency field in Fig. 5b are about a quarter-wavelength east of the low-frequency wave itself. The mixed-in waves are also visible on the time mean tendency maps calculated in the moving frames with $m = 2$ and $m = 3$ but become small for $m = 4$.

One needs to be reminded here that the maps shown in Figs. 2–5 are obtained directly from the wind data without making use of the vorticity equation. That the time mean tendency maps are nearly orthogonal to those of the low-frequency anomaly surely warrants the statement that low-frequency transients, by and large, are mobile waves. Without use of the vorticity equation, the phase-shifting method enables us to extract only the overall propagating tendency components of low-frequency anomaly. Another way of saying the same is that in the mean the net amplifying tendency must be very small. However, an individual tendency component induced by a particular interaction term in the vorticity equation (e.g., feedback of high-frequency eddies) may exhibit a good projection onto the time-mean maps of low-frequency transients if the corresponding physical process systematically provides/draws energy to/from low-frequency transients. As we shall see below, the phase-shifting method indeed enables us to identify the terms that contribute amplifying/maintenance/decaying part of the total tendency.

Now we want to examine the contribution of an individual tendency component defined on the rhs of Eq. (5) to the observed tendency as viewed from the four moving frames. For the sake of brevity, we present in Fig. 6 only the time mean maps calculated from the frame moving with $m = 1$, the same moving frame that yields the maps presented in Fig. 2. The results obtained with $m = 1$ can be qualitatively generalized to the results obtained in the frames with $m = 2$, $m = 3$, and $m = 4$. We will point out the few major differences between the results obtained with $m = 1$ and those with other values of m and the implication of the differences along with the presentation of the results in Fig. 6.

Figure 6 consists of 12 maps, all of which are obtained in one moving frame ($m = 1$) so that there should be no ambiguity in comparing the 12 maps. Panels (a) and (b) have already been shown in Fig. 2; they reappear here just for the sake of an easy comparison in the same format. Panel (c) is the mean map of the sum of all the calculated tendency components χ_j, where j runs from 1 to 8. Loosely speaking, the large-scale features on the map in panel (c) are more or less in the same positions as those of the observed tendency [panel (b)]. The amplitude of the sum of the calculated tendencies, however, is about twice as large as that of the observed tendency (for which we have offered a tentative explanation in section 4). The resemblance between the sum of the calculated tendencies and the observed tendency would suggest that the vorticity equation (3) is, in the mean, capable of capturing a large portion of the changes in low-frequency wave transients. The finding of the similarity between panels (b) and (c) and the large amplitude of the residue term [panel (d)] is quite consistent with the fact that the correlation shown in Fig. 1a is positive but below 0.8 everywhere. It is also seen that the residue term [panel (d)] has a very large (negative) projection on the low-frequency wave itself [panel (a)]. This would strongly suggest that the inclusion of some types of simple linear damping in Eq. (3) is well justifiable and can improve

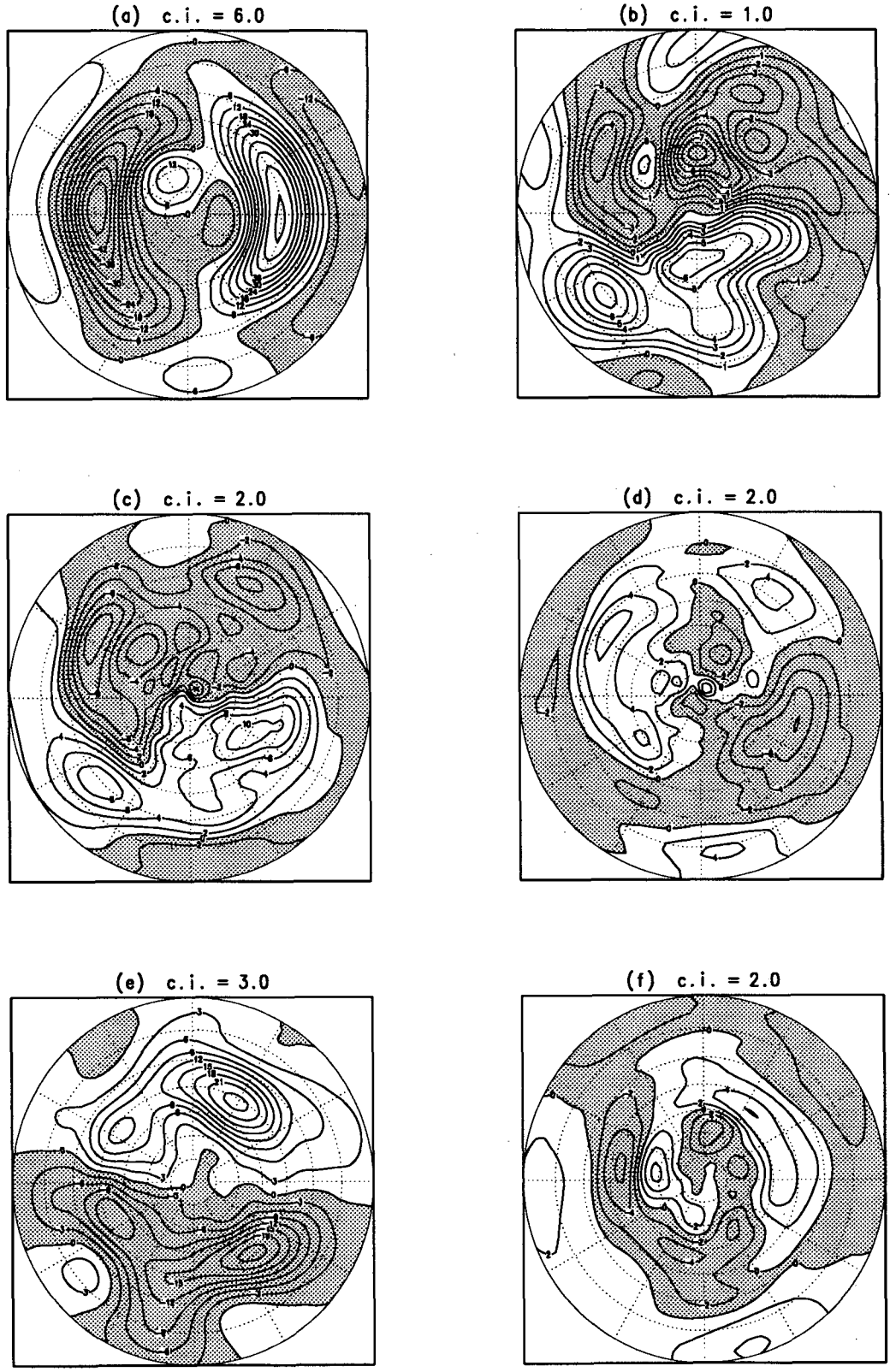

FIG. 6. Time mean maps calculated in the moving frame $m = 1$: (a) the low-frequency streamfunction; (b) the observed tendency of the low-frequency streamfunction; (c) sum of the calculated tendency components; (d) residue

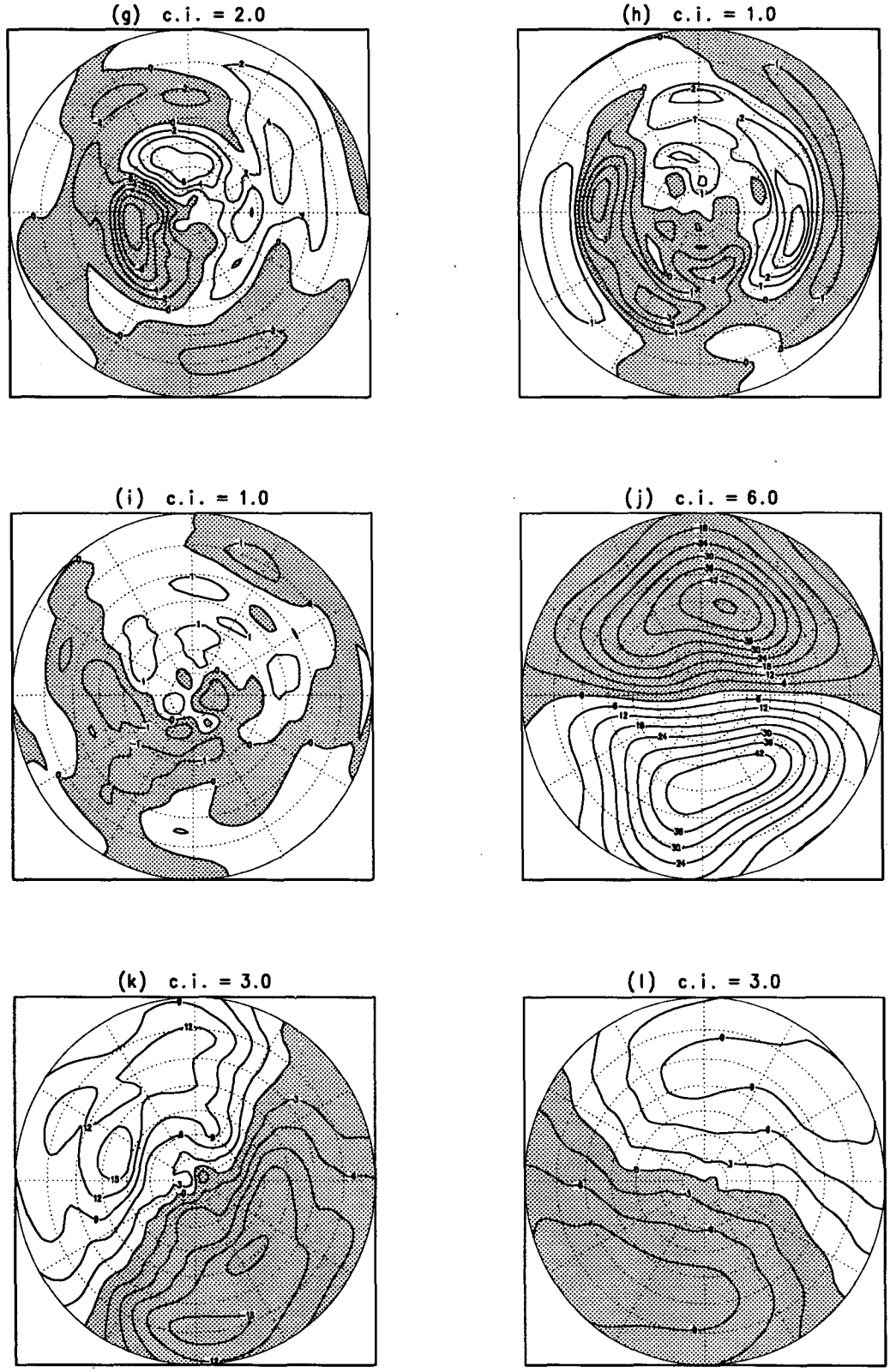

FIG. 6. (*Continued*) term; panels (e)–(l) are χ_j, $j = 1, 2, \cdots, 8$, respectively. The unit for (a) is 10^5 m^2 s^{-1} and for (b)–(l) is m^2 s^{-2}. The area with negative values has been shaded.

the quantitative agreement between panel (b) and panel (c) of this figure.

The remaining eight panels of Fig. 6 are the mean maps of the individual tendency component χ_j defined in Eq. (6) for $j = 1, 2, 3, 4, 5, 6, 7$, and 8. Consistent with Table 1, the tendency components χ_1 and χ_6 are the leading terms among the eight components. It is not surprising to see that the zonally symmetric part of the climatological flow tends to move low-frequency waves eastward[1] [χ_1 in panel (e)] whereas the beta effect tends to move low-frequency waves westward [χ_6 in panel (j)]. For the longer waves ($m = 1$, 2, and 3), the beta effect is stronger than the advection of low-frequency relative vorticity by the zonal mean wind of the climatological flow, so in the mean the longer waves travel westward. In the case of $m = 4$, the amplitude of the χ_1 is larger than that of χ_6. As a result, the low-frequency wave $m = 4$ in the mean moves toward the east. These results are broadly consistent with the classical theory of Rossby waves (Rossby 1939). In the moving frame, the net sum of χ_1 and χ_6 more or less resembles χ_0, which can be calculated directly from the observation without utilizing the vorticity equation.

Beside χ_1 and χ_6, the tendency component χ_7 [panel (k)], the tendency due to the stretching/divergent effect of the irrotational wind, also appears to be an important factor in determining the traveling speed of low-frequency waves. This term always acts to compensate part of the tendency induced by the beta effect and tends to make low-frequency waves move less westward. The relation between χ_6 and χ_7 can be easily explained by the classic Rossby wave theory since the χ_7 is related to the Rossby deformation radius in the dispersion relation for the barotropic Rossby wave in a shallow-water system, which acts to reduce the westward Rossby wave's phase speed (e.g., Pedlosky 1987). The tendency component due to the ageostrophic effect (χ_8), being the fourth largest term among the eight tendency components for $m = 1$, also acts to retard the westward propagation of the low-frequency wave $m = 1$. However, this term becomes negligible compared to other tendency components on the mean maps derived in the moving frames with $m = 2$, 3, and 4 (not shown here).

Among the eight tendency components, only χ_2 and χ_4 act to reinforce low-frequency waves for $m = 1$, 2, 3, and 4. As seen from Fig. 6, the mean tendency components χ_2 and χ_4 [panel (f) and (h)] are almost in phase with the low-frequency wave itself [panel (a)]. The in-phase relation of χ_4 (the tendency induced by the vorticity flux of the high-frequency eddies) with low-frequency flow has been well documented in the literature and has been one of the focal points in understanding the internal dynamics of the midlatitude atmospheric low-frequency variability (see references cited in the introduction). The finding of the nearly in-phase relation of χ_2 (the tendency induced by interaction of the stationary waves and low-frequency transients) with low-frequency waves is relatively new in the literature. Nevertheless, the spatially coherent relation between χ_2 and low-frequency waves is quite explainable from the well-known barotropic instability theory of zonally asymmetric time mean flow (e.g., Simmons et al. 1983). From an energetics point of view, the nearly in-phase relation between χ_2 (or χ_4) and low-frequency waves implies a net kinetic energy conversion from stationary waves (or from high-frequency eddies) to low-frequency waves. This interpretation is supported by our energetics calculation (not shown here), which reveals two barotropic energy sources for low-frequency transients in the Northern Hemisphere: (i) the energy conversion from the zonally asymmetric part of the climatological flow and (ii) the energy generation due to the downgradient momentum flux of high-frequency eddies.

The mean map of the tendency component due to the self-interaction of low-frequency transients (χ_3) calculated in the moving frame $m = 1$ seems to have a positive projection on the low-frequency wave itself (Fig. 6g vs Fig. 6a) and a negative projection on the observed tendency (Fig. 6g vs Fig. 6b). This means that in the mean χ_3 acts to reinforce the low-frequency wavenumber one and to retard its westward traveling speed. Since the tendency component χ_3 is a result of the nonlinear interactions of low-frequency transients themselves, the energy source for reinforcing the low-frequency wavenumber one by χ_3 has to come from the low-frequency waves with a shorter spatial scale, which essentially is an upscale energy cascade process. The mean map of χ_3 calculated with $m = 2$ also shows somewhat positive projection on the low-frequency wave $m = 2$ (not shown here). But the mean maps of χ_3 calculated with $m = 3$ and $m = 4$ (not shown here) exhibit nearly orthogonal patterns to the corresponding low-frequency waves. Hence, the tendency component due to the self-interaction of low-frequency transients contributes more to the propagation part of the low-frequency waves as the wavenumber increases.

The only remaining term in Eq. (5) that has not been discussed so far is the tendency component due to the interaction between low- and high-frequency transients (χ_5). Unlike other mean maps presented in this figure, the mean map of χ_5 does not appear to have obvious statistical or physical significance because of the smallness of the amplitude and the irregular patterns on the map. The mean maps of χ_5 calculated with other values of m reveal the same finding. This implies that in a statistical sense, χ_5 has no spatially coherent relation

[1] Additional calculation reveals that the advection of the low-frequency vorticity by the zonally averaged climatological wind has a much larger contribution to the mean map of χ_1 than the advection of the zonally averaged climatological vorticity by the low-frequency wind [see the definition of χ_1 in (6) for a reference].

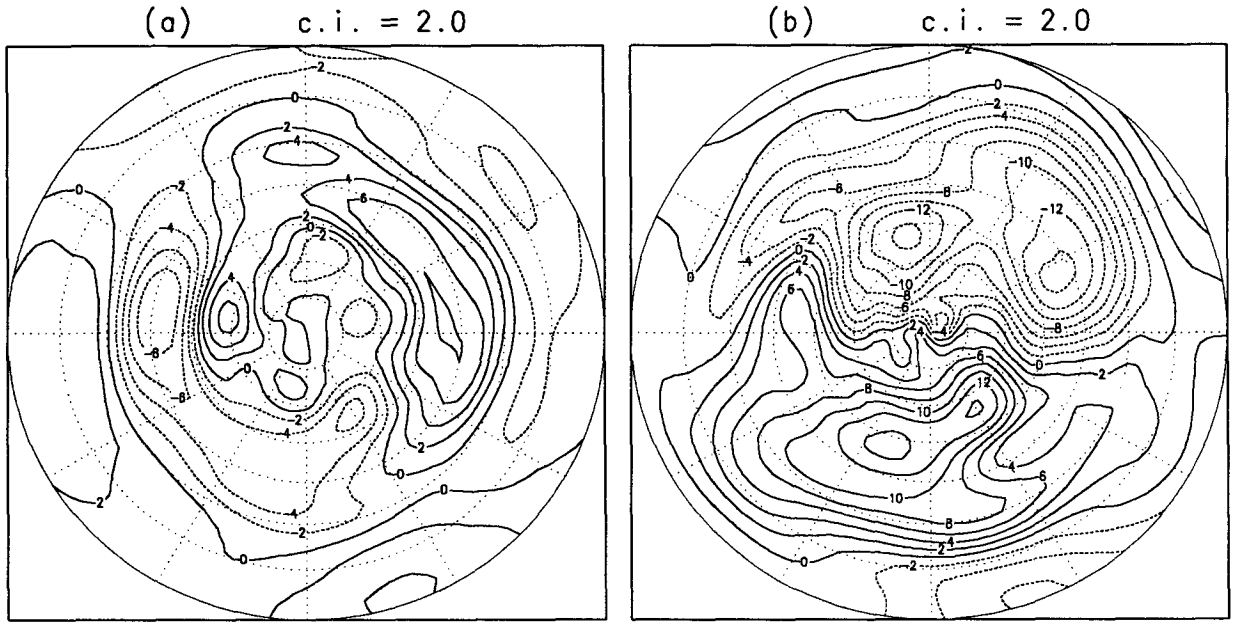

FIG. 7. Time-mean maps calculated in the moving frame $m = 1$: (a) $(\chi_2 + \chi_4)$ and (b) $(\chi_1 + \chi_6 + \chi_7 + \chi_8)$. The unit is $[m^2 s^{-2}]$.

either with the low-frequency flow or with its tendency. Hence, χ_5 acts more like a random process to low-frequency transients with a small mean but nontrivial variability (according to Table 1, the variability of χ_5 is as large as that of χ_4). In the mean, it contributes neither particularly to propagation of low-frequency waves nor to maintenance of low-frequency transients.

To gain an idea of the net effect of the maintenance and propagation tendency components, we present in Figs. 7–10 the time mean map of $(\chi_2 + \chi_4)$ in panel (a) and time mean map of $(\chi_1 + \chi_6 + \chi_7 + \chi_8)$ in panel (b) for the moving frames with $m = 1$, through 4, respectively. We do not include χ_3 on either of the two maps because this term, representing an upscale

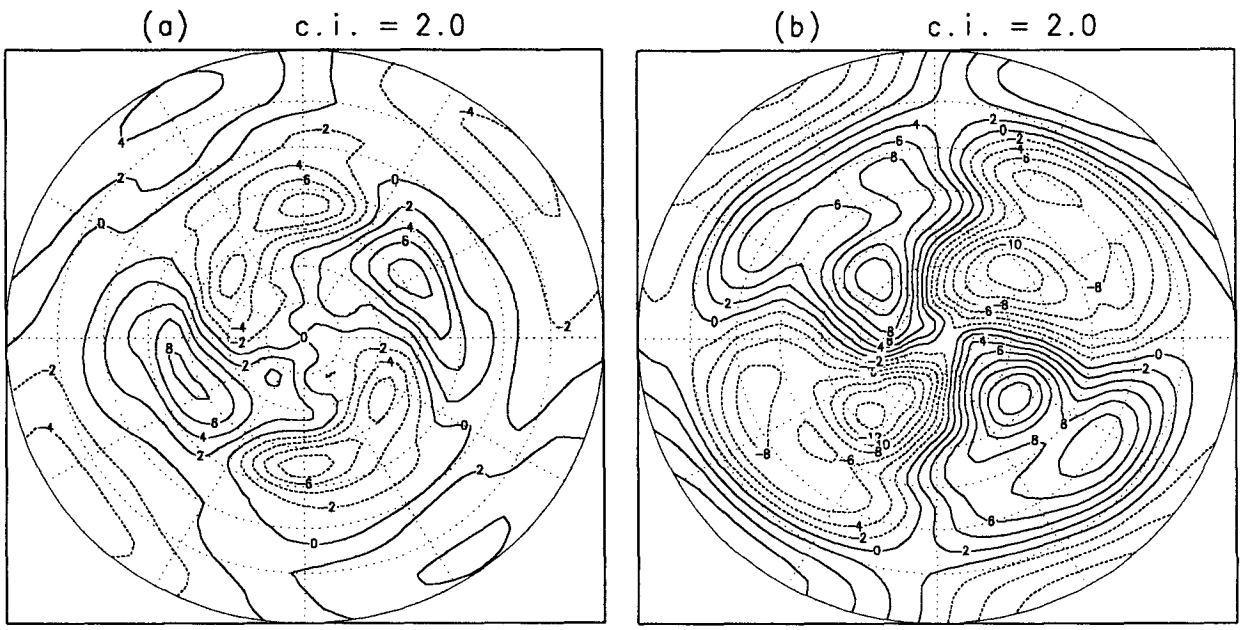

FIG. 8. As in Fig. 7 except for the moving frame $m = 2$.

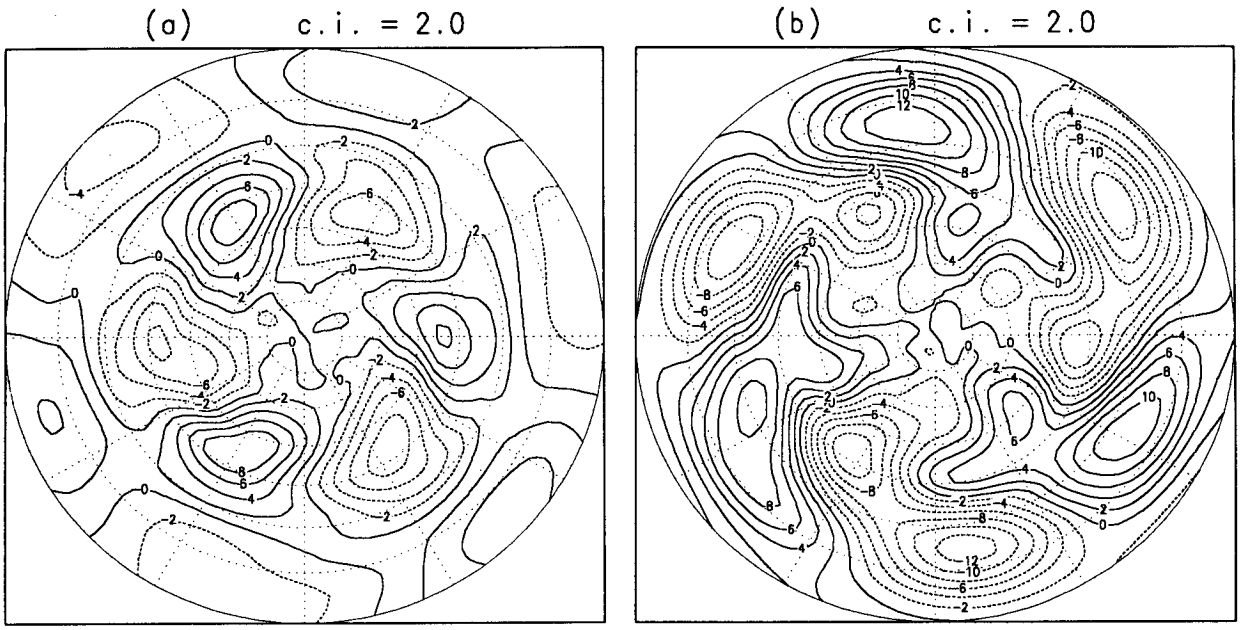

FIG. 9. As in Fig. 7 except for the moving frame $m = 3$.

energy cascade process among low-frequency waves themselves, is mixed with maintenance and propagation effects for $m = 1$ and 2 and contributes largely to propagation for $m = 3$ and 4. Exclusion of χ_5 in these figures is because of its statistical insignificance. The resemblance of panel (a) of Fig. 7 (or Fig. 8, Fig. 9, or Fig. 10) with panel (a) of Fig. 2 (or Fig. 3, Fig. 4, or Fig. 5) clearly indicates the net maintenance effect of the tendency components χ_2 and χ_4 on the low-frequency transients. The good spatial correlation between the map shown in Fig. 7b (or Fig. 8b, Fig. 9b, or Fig. 10b) and the map in Fig. 2b (or Fig. 3b, Fig. 4b, or Fig. 5b) suggests that the four tendency terms χ_1, χ_6, χ_7, and χ_8 capture a large portion of the propagation

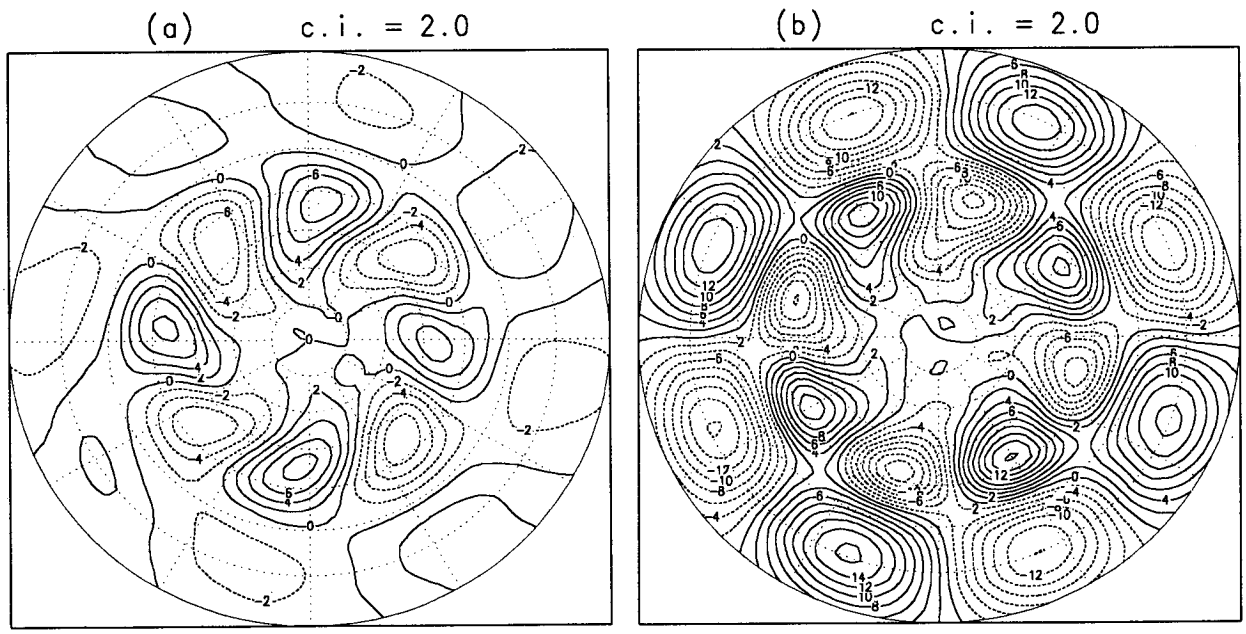

FIG. 10. As in Fig. 7 except for the moving frame $m = 4$.

part in the observed tendency.[2] Another important message in Figs. 7–10 is that the net effect of propagation tendency components is no longer overwhelming the maintenance tendency components due to a great deal of cancellation among the various propagation tendency components.

6. Summary and discussion

This paper reports a diagnostic analysis with the ECMWF wind data on the low-frequency component of 500-mb circulation in terms of the tendency components of low-frequency streamfunction induced by all terms in the framework of the vorticity equation. Specifically, we have calculated eight tendency components of the 500-mb low-frequency streamfunction on the basis of the vorticity equation for low-frequency flow [see Eq. (5) for the definitions]. We then compared each of the tendency components with the (total) observed tendency of the low-frequency streamfunction and the low-frequency streamfunction itself. By doing this, we are able to distinguish the internal interactions that primarily act to make low-frequency waves propagate from those that are mostly responsible for maintenance of low-frequency transients.

The two largest tendency components are the tendency (denoted as χ_1) induced by the advection of low-frequency transients by the zonally symmetric component of the time-mean flow and the tendency (denoted as χ_6) due to the advection of the planetary vorticity by low-frequency transients (or beta effect). These two terms exclusively contribute to the propagation part of the tendency of low-frequency waves. One produces eastward propagation (χ_1) and the other westward propagation (χ_6). In addition to these two large terms, the tendency components due to the self-interaction among low-frequency transients (χ_3) and the stretching/converging effect of the nonrotational flow (χ_7) also primarily act to make low-frequency waves move eastward. The sum of these four tendency components more or less determines the propagation part in the observed tendency field of the low-frequency streamfunction. The tendency due to the ageostrophic effect (χ_8) appears to be important only for the very longest low-frequency wave and primarily retards the westward phase speed of the longest wave. In summary, the propagation is primarily determined by a balance between χ_1 and χ_6, with further slowdown (for the westward propagating waves) action coming from χ_3, χ_7, and χ_8. While χ_3, χ_7, and χ_8 are smaller, they are vital in making the low-frequency waves be low frequency.

There are only two tendency components that mainly contribute to the maintenance of low-frequency waves. One is due to the interaction of low-frequency transients and stationary waves (χ_2); the other results from the vorticity flux by high-frequency eddies (χ_4). The term χ_4 is a familiar one and has been examined in many studies to account for the nonlinear interaction relation between low- and high-frequency eddies. The amplifying tendency resulting from the interaction of low-frequency transients and stationary waves is another way of viewing the barotropic instability theory of the zonally asymmetric time mean flow. The self-interaction among low-frequency transients themselves (i.e., χ_3) also acts as an additional energy source for the longer low-frequency waves through the upscale energy cascade process.

The findings of these three (mainly two) mechanisms that contribute to the maintenance part of the low-frequency waves agree with the results of Branstator's linear forcing response study (1992). However, we further demonstrate here that these three mechanisms work well for the mobile low-frequency variability, not just for geographically standing variations as captured in an EOF analysis. Hence, we add that the interaction between low-frequency transients and the zonally asymmetric part of the time mean flow is responsible for maintenance of not only the standing oscillatory low-frequency patterns but also the mobile low-frequency waves.

The tendency component due to the cross interaction between low- and high-frequency eddies (χ_5) appears to have a spatially incoherent relation with both the low-frequency flow and its tendency. Hence, this term acts more like a random process in the evolution of low-frequency flow with small but nontrivial variability.

We note that the amplitude of the tendency components that are responsible for the maintenance of low-frequency waves is much smaller than an individual propagation tendency component. Particularly, the tendency component arising from the vorticity flux of high-frequency eddies, which has been examined extensively in the literature regarding the internal forcing mechanism of low-frequency variations by high-frequency eddies, is actually one of the smallest terms in the tendency equation. Nevertheless, because there is a great deal of cancellation among the different propagating tendency components, the net effect of all propagating tendency components is just slightly stronger than the sum of maintenance tendency components.

Our study on the tendency of low-frequency variability suggests that a large portion of the low-fre-

[2] Theoretically speaking, we can only say that χ_6 is purely a propagation tendency component and the rest of χ_j is a mix of both propagation and maintenance. For an example, the sum of χ_2 and χ_4 for $m = 2$ has somewhat significant projection on the propagation component of the tendency (Fig. 8a vs Fig. 3b). Also the sum of χ_1, χ_6, χ_7, and χ_8 for $m = 3$ [panel (b) of Fig. 9] appears to show a damping effect on the low-frequency wave $m = 3$ (Fig. 9b vs Fig. 4a). Therefore, here we only make an empirical statement that a large portion of χ_2 and χ_4 (or χ_1, χ_6, χ_7, and χ_8) can be related to the maintenance (or propagation) tendency component of the low-frequency transients.

quency variability is due to propagation of planetary-scale waves. Clearly, the characteristics of propagation do not imply that low-frequency waves are "free" waves. Our study indicates that the nonlinear interaction of disturbances with different time scales is an important (perhaps the only) energy source for low-frequency variability. In this regard, the low-frequency transients are internally "forced," slowly propagating mobile waves, hence placing a heavy burden on extended-range forecast models to correctly forecast both advection and maintenance.

Another important implication of our study is that the nonlinear shallow-water vorticity equation with some types of simple linear damping mechanisms is, in the mean, capable of capturing a significantly large portion of the evolution of the low-frequency wave transients. This provides an observational basis for a nonlinear dynamic model for low-frequency transients only. The key is to parameterize the coherent and noncoherent effects of high-frequency transients (χ_4 and χ_5, respectively) on low-frequency transients as well as the dissipation terms.

Acknowledgments. This research was supported in part by NSF Grant ATM-9103647 and by NOAA Grant NA89-AA-H-MC066. Part of the computations were performed on the Cray Y-MP supercomputer at the National Center for Atmospheric Research. The suggestions from the two anonymous reviewers have led to significant improvement of the presentation and are much appreciated.

REFERENCES

Blackmon, M. L., 1976: A climatological spectral study of the 500 mb geopotential height of the Northern Hemisphere. *J. Atmos. Sci.,* **33,** 1607–1623.

——, J. M. Wallace, N. C. Lau, and S. L. Mullen, 1977: An observational study of the Northern Hemisphere wintertime circulation. *J. Atmos. Sci.,* **34,** 1040–1053.

Branstator, G., 1992: The maintenance of low-frequency atmospheric anomalies. *J. Atmos. Sci.,* **49,** 1924–1945.

Cai, M., and H. M. van den Dool, 1991: Low-frequency waves and traveling storm tracks. Part I: Barotropic component. *J. Atmos. Sci.,* **48,** 1420–1436.

——, and ——, 1992: Low-frequency waves and traveling storm tracks. Part II: Three-dimensional structure. *J. Atmos. Sci.,* **49,** 2506–2524.

Green, J. S. A., 1977: The weather during July 1976: Some dynamical considerations of the drought. *Weather,* **32,** 120–126.

Higgins, R. W., and S. D. Schubert, 1993: Low-frequency synoptic-eddy activity in the Pacific storm track. *J. Atmos. Sci.,* **50,** 1672–1690.

Holopainen, E., and C. Fortelius, 1987: High-frequency transient eddies and blocking. *J. Atmos. Sci.,* **44,** 1632–1645.

Hoskins, B. J., I. N. James, and G. H. White, 1983: The shape, propagation and mean-flow interaction of large-scale weather systems. *J. Atmos. Sci.,* **40,** 1595–1612.

Lau, N. C., 1978: On the three-dimensional structure of the observed transient eddy statistics of the Northern Hemisphere wintertime circulation. *J. Atmos. Sci.,* **35,** 1900–1923.

——, 1988: Variability of the observed midlatitude storm tracks in relation to low frequency changes in the circulation pattern. *J. Atmos. Sci.,* **45,** 2718–2743.

——, and J. Nath, 1991: Variability of the baroclinic and barotropic transient eddy forcing associated with monthly changes in the midlatitude storm tracks. *J. Atmos. Sci.,* **48,** 2589–2613.

——, and E. O. Holopainen, 1984: Transient eddy forcing of the time-mean flow as identified by geopotential tendencies. *J. Atmos. Sci.,* **41,** 313–328.

Mak, M., and M. Cai, 1989: Local barotropic instability. *J. Atmos. Sci.,* **46,** 3289–3311.

Metz, W., 1989: Low-frequency anomalies of atmospheric flow and the effects of cyclone-scale eddies: A canonical correlation analysis. *J. Atmos. Sci.,* **46,** 1026–1041.

——, 1990: Empirical modeling of extratropical cyclone vorticity fluxes. *Tellus,* **42A,** 14–27.

——, 1991: Optimal relationship of large-scale flow patterns and the barotropic feedback due to high-frequency eddies. *J. Atmos. Sci.,* **48,** 1141–1159.

Pedlosky, J., 1987: *Geophysical Fluid Dynamics.* second ed. Springer-Verlag, 710 pp.

Rossby, C. G., 1939: Relation between variations in the intensity of the zonal circulation of the atmosphere and the displacements of the semi-permanent centers of action. *J. Mar. Res.,* **2,** 38–55.

Shutts, G. J., 1983: The propagation of eddies in diffluent jetstreams: Eddy vorticity forcing of 'blocking' flow fields. *Quart. J. Roy. Meteor. Soc.,* **109,** 737–761.

Simmons, A. J., J. M. Wallace, and G. W. Branstator, 1983: Barotropic wave propagation and instability, and the atmospheric teleconnection patterns. *J. Atmos. Sci.,* **40,** 1369–1392.

Van den Dool, H. M., 1982: What do observations tell about long-range predictability? *On the Theory and Application of Simple Climate Models to the Problem of Long Range Weather Prediction,* R. Mureau, C. J. Kok, and R. J. Haarsma, Eds., Koninklijk Nederlands Meteorologisch Instituut Workshop, 129 pp.

Wallace, J. M., and M. L. Blackmon, 1983: Observations of low-frequency atmospheric variability. *Large-Scale Dynamical Processes in the Atmosphere,* B. J. Hoskins and R. P. Pearce, Eds., Academic Press, 397 pp.